



HHS Public Access

Author manuscript

Nat Methods. Author manuscript; available in PMC 2012 May 01.

Published in final edited form as:

Nat Methods. ; 8(11): 933–935. doi:10.1038/nmeth.1716.

Gas-phase purification enables accurate, large-scale, multiplexed proteome quantification with isobaric tagging

Craig D Wenger¹, M Violet Lee^{1,3}, Alexander S Hebert^{2,3}, Graeme C McAlister¹, Douglas H Phanstiel¹, Michael S Westphall³, and Joshua J Coon^{1,2,3}

¹Department of Chemistry, University of Wisconsin–Madison, Madison, Wisconsin, USA

²Department of Biomolecular Chemistry, University of Wisconsin–Madison, Madison, Wisconsin, USA

³Genome Center of Wisconsin, University of Wisconsin–Madison, Madison, Wisconsin, USA

Abstract

We describe a mass spectrometry method, QuantMode, which improves the accuracy of isobaric tag-based quantification by alleviating the pervasive problem of precursor interference—co-isolation of impurities—through gas-phase purification. QuantMode analysis of a yeast sample ‘contaminated’ with interfering human peptides showed substantially improved quantitative accuracy compared to a standard scan, with a small loss of spectral identifications. This technique will allow large-scale, multiplexed quantitative proteomics analyses using isobaric tagging.

Protein identification technologies have rapidly matured such that constructing catalogs of the thousands of proteins present in a cell using mass spectrometry is now relatively straightforward¹. Knowing how the abundance of these molecules change under various circumstances, however, is not straightforward². Stable isotope labeling by amino acids in cell culture (SILAC) provides a means to make binary or ternary comparisons of different samples via metabolic labeling^{3,4}. By interlacing these two- or three-way measurements, higher-order comparisons can be obtained⁵. Such experiments are invaluable; however, constructing this type of multi-faceted proteomics study is a time-intensive undertaking.

Isobaric tagging^{6,7} is an elegant solution to this problem, allowing relative quantification of up to eight proteomes simultaneously^{8,9}. Further, unlike metabolic labeling approaches, it is compatible with mammalian tissues and biofluids. Despite its potential, isobaric tagging has

Users may view, print, copy, download and text and data-mine the content in such documents, for the purposes of academic research, subject always to the full Conditions of use: http://www.nature.com/authors/editorial_policies/license.html#terms

Correspondence should be addressed to J.J.C. (jcoon@chem.wisc.edu).

Note: Supplementary information is available on the Nature Methods website.

AUTHOR CONTRIBUTIONS

C.D.W. designed research, performed research, and wrote the paper; M.V.L. designed research and performed research; A.S.H. designed research and performed research; G.C.M. designed research and performed research; D.H.P. designed research; M.S.W. designed research and wrote the paper; J.J.C. designed research and wrote the paper.

COMPETING INTERESTS STATEMENT

The authors declare competing financial interests: Two patent applications, in part related to this manuscript, are pending. US Serial Numbers 13/086638 (inventors Wenger CD, Phanstiel DP, and Coon JJ) and 61/471461 (inventors Coon JJ and Westphall MS).

not been widely embraced for large-scale studies¹⁰—chiefly because of the problem of precursor interference. This problem does not exist for SILAC because abundance measurements are obtained from high-resolution survey mass spectra (MS^1). Even for very complex samples having hundreds of co-eluting peptides, high-resolving power mass analyzers can easily distinguish the target from neighboring peaks less than 0.01 Th away.

In the isobaric tagging approach, the target peptide is isolated at much lower resolution (typically 1–3 Th), then dissociated to produce reporter tags. Therefore, the quantitative signal in the reporter region is compiled from every species in the isolation window¹¹. For highly complex mixtures, co-isolation of multiple species is the rule, not the exception (*vide infra*). This can compromise quantitative accuracy, as measured ratios tend to be compressed toward the median ratio of 1:1, and thus has restricted isobaric tagging to applications with relatively low sample complexity.

To document the extent of precursor interference, we created a *precursor purity model* (Supplementary Fig. 1) by labeling tryptic yeast peptides with the tandem mass tag 6-plex with reporter ion at nominal m/z 126 (TMT⁶-126) isobaric tag. We combined these peptides with tryptic human peptides which had been labeled with the TMT⁶-131 tag. By incorporating human peptides as the ‘interference’, we effectively modeled the precursor contamination characteristic of a human proteomic analysis. Following nanoflow liquid chromatography–tandem mass spectrometry (nLC–MS/MS), using a standard higher-energy collisional dissociation (HCD) method, we examined the reporter m/z regions of MS/MS spectra that were uniquely mapped to yeast. On average, only 68% of reporter ion signal originated from the target peptide (Fig. 1a). Only 3% of MS/MS spectra were derived from ultrapure (99%) precursors.

We next wondered: what effect does this prevalent interference have on isobaric tag–based quantification? To address this question, we created a *quantitative accuracy model* (Supplementary Fig. 2) by labeling tryptic yeast peptides with TMT⁶ tags and mixing them in ratios of 10:1:3:2:5:1.5. We combined this sample with an equal mass of tryptic human peptides, also labeled with TMT⁶ but mixed in ratios of 1:1:1:1:1:1. We assessed the degradation of quantitative accuracy by examining reporter ion ratios in yeast peptide spectra. This represented the worst-case interference scenario because we analyzed this mixture directly with nLC–MS/MS without prior fractionation. Shockingly, the yeast 10:1 ratio was measured at a median of 4.4:1—a 2.3-fold underestimation or a 66% relative error (Fig. 1b, Supplementary Fig. 3a–d, Supplementary Table 1).

One obvious approach to reduce interference is to narrow the MS/MS isolation width so that fewer contaminant ions are present during precursor activation. However, applying this approach produced only minor improvements (4.3:1 to 5.4:1 for 3 to 1 Th, Supplementary Fig. 4). Note that isolation is less effective as window widths narrow, resulting in fewer identifications (3,348 to 1,723 yeast PSMs for 3 to 1 Th). Chromatographic pre-fractionation did not reduce ratio truncation relative to an unfractionated analysis (unfractionated: 4.4:1 versus fractionated: 4.3:1, Supplementary Fig. 5 and Supplementary Table 1).

Another strategy is to reject quantitative information from precursors having interference above a specified threshold. For the above dataset, we used post-acquisition filtering (PAF)—an option in TagQuant of COMPASS¹²—to remove MS/MS spectra if the precursor's purity was below 75% within the 3 Th MS/MS isolation window of the preceding MS¹ spectrum. This technique (Fig. 1b, middle boxplot) improves quantification (to 6.2:1), but comes at the expense of 66% of the data: 3,098 versus 1,068 quantified yeast PSMs. We devised a method, real-time filtering (RTF, Supplementary Note), to execute this logic in real time so that only precursors without major interference were sampled (Supplementary Fig. 6). RTF boosts quantifiable PSMs relative to PAF and yields comparable accuracy (Supplementary Fig. 7 and Supplementary Table 1). However, as the correct 10:1 ratio was still not achieved, these data evince that background contaminants are not always detectable.

We therefore devised a fresh approach to combat interference directly via gas-phase purification: that is, by deconvolving the co-isolated contaminants from the precursor in m/z space by manipulating either mass or charge before performing a second isolation. Expedient proton-transfer ion/ion reactions (PTR)¹³ efficiently reduce ion charge state and can be integrated easily into instrument control methods. And because ion/ion reactions can be conducted on a variety of instruments, including ion traps, ion trap hybrids (i.e., orbitrap and FT-ICR), and quadrupole–time-of-flight (Q-TOF)¹⁴ mass spectrometers, this approach should be broadly accessible. Note that standalone ion trap systems, which are capable of performing beam-type collision-activated dissociation (CAD)¹⁵, are wholly compatible with the approach presented here—such a combination should offer a benchtop solution to multiplexed quantification.

Consider a doubly charged precursor at 500 Th co-isolated with a triply charged contaminant also at 500 Th. Following PTR, the precursor is now positioned at m/z 999 (+1), whilst the interfering species is moved to m/z 749.5 (+2). Subsequent isolation of m/z 999 yields a purified precursor population from which to generate accurate quantification. In essence, this facilitates isolation on the basis of both m/z and z rather than simply m/z . Contaminants having charge identical to the precursor are still spread in m/z space; for example, a +2 interference at m/z 501 will be transformed to m/z 1001 and effectively eliminated from the second isolation window (997.5–1000.5 Th).

We devised a scan function to implement this concept, which we call QuantMode, comprising the following steps (Supplementary Fig. 8 and Supplementary Protocol): (1) first cation injection (quadrupole linear ion trap, QLT), (2) first cation precursor isolation (QLT), (3) anion injection (QLT), (4) PTR (QLT), (5) charge-reduced precursor isolation (QLT), (6) HCD of the charge-reduced precursor (HCD cell), (7) transfer of HCD products (c-trap), (8) second cation injection (QLT), (9) second cation precursor isolation (QLT), (10) resonant-excitation collision-activated dissociation (CAD, QLT), (11) transfer CAD products (c-trap), (12) transfer HCD/CAD products (orbitrap), and (13) mass analysis of reporter and sequence ions together (orbitrap).

The purifying effects of QuantMode are evident in Figure 2. Examination of a 3 Th precursor isolation window (m/z 595.72, +3) from the preceding MS¹ scan reveals extensive contamination—merely 49% purity. This impurity does not hinder sequence identification

upon HCD (peptide sequence RINELTLLVQK, OMSSA expectation value 2×10^{-10}). It does, however, cripple quantitative accuracy: the 10:1 true value is recorded as 2.5:1. A 30 ms PTR step on this impure population efficiently deconvolves the target (~45% for +3→+2). The doubly protonated precursor (893.08 Th) is then isolated from the contaminants (85% purity); note this mass analysis following PTR, while illustrative, is not necessary, as the precursor's charge-reduced m/z is easily calculated. This untainted charge-reduced precursor population is then dissociated under HCD conditions favorable to reporter ion generation, the products of which are stashed in the c-trap. Next, sequence-informative products are formed through re-injection of the original triply charged precursor (m/z 595.72), isolation, and fragmentation in the QLT. After combination in the c-trap, the mixed ion population is mass analyzed in the orbitrap. The QuantMode scan, like its HCD-only counterpart, yields a high-confidence match to the same peptide (OMSSA expectation value 2×10^{-8}). Yet in stark contrast to the truncated 2.5:1 ratio, QuantMode obtains a 9.9:1 ratio, virtually equivalent to the expected 10:1.

The QuantMode scan affords manifold benefits. First, independent control of dissociation parameters can simultaneously improve quantitative accuracy and spectral identifications (Supplementary Fig. 9). Second, decoupling permits the use of isobaric tagging with otherwise incompatible dissociation methods (for example, resonant-excitation CAD, electron-capture or electron-transfer dissociation, etc.), allowing optimal identification and application of isobaric tagging to diverse sample types. Third, beyond decoupling benefits, QuantMode elegantly combines multiple disparate steps into a single scan to improve duty cycle.

To validate the efficacy of this method we re-analyzed the mixed organism models with QuantMode. For the *precursor purity model*, purity improved from 68% to 88% among the same 1,297 precursors. Even more striking is the surge in ultrapure (99%) precursors—from 3% to 23%. But does this enhanced purity translate to quantitative accuracy? Yes: applying QuantMode to analyze the *quantitative accuracy model* shifted the measured ratio from 4.4:1 with HCD to 8.5:1, much nearer to the true value of 10:1 (Fig. 1b, Supplementary Fig. 3a–d, Supplementary Table 1). QuantMode incurs a 21% loss (3,098 to 2,459) in identified yeast PSMs; however, all are suitable for quantification. Outliers are more frequently observed with QuantMode, partly attributable to its increased dynamic range and better overall precision, and to a lesser extent residual impurities and occasional inaccurate precursor charge state assignment, which results in incorrect isolation of the charge-reduced product.

We have demonstrated that isobaric tagging suffers from systemic loss of quantitative accuracy on account of pervasive and inherent precursor interference. QuantMode mitigates this problem through gas-phase purification and substantially increases quantitative accuracy without severely penalizing identifications. The method facilitates multiplexed measurements of protein and post-translation modification dynamics, as well as biological replicates for proper statistical treatment. This initial implementation will doubtless evolve to include a repertoire of dissociation methods, enhancing both sequence and reporter ion generation, and to improve duty cycle.

METHODS

Methods and any associated references are available in the online version of the paper at <http://www.nature.com/naturemethods/>.

Supplementary Material

Refer to Web version on PubMed Central for supplementary material.

Acknowledgments

We thank A.J. Bureta for figure illustrations, A. Williams for critical proofreading, A. Ledvina and D. Bailey for assistance with instrument firmware code modifications, S. Hubler for theoretical calculations regarding yeast and human peptides, and J. Brumbaugh and J. Thomson for culturing the human cells. We thank J. Syka, J. Schwartz, V. Zabrouskov, J. Griep-Raming, and D. Nolting (all of Thermo Fisher Scientific) for helpful discussions. This work was supported by the National Institutes of Health grant R01 GM080148 to J.J.C. D.H.P. acknowledges support from an NIH predoctoral traineeship—the Genomic Sciences Training Program, NIH 5T32HG002760.

References

1. de Godoy LMF, et al. *Nature*. 2008; 455:1251–1255. [PubMed: 18820680]
2. Ong SE, Mann M. *Nat Chem Biol*. 2005; 1:252–262. [PubMed: 16408053]
3. Jiang H, English AM. *J Proteome Res*. 2002; 1:345–350. [PubMed: 12645890]
4. Ong SE, et al. *Mol Cell Proteomics*. 2002; 1:376–386. [PubMed: 12118079]
5. Olsen JV, et al. *Sci Signal*. 2010; 3:ra3. [PubMed: 20068231]
6. Thompson A, et al. *Anal Chem*. 2003; 75:1895–1904. [PubMed: 12713048]
7. Ross PL, et al. *Mol Cell Proteomics*. 2004; 3:1154–1169. [PubMed: 15385600]
8. Choe L, et al. *Proteomics*. 2007; 7:3651–3660. [PubMed: 17880003]
9. Dayon L, et al. *Anal Chem*. 2008; 80:2921–2931. [PubMed: 18312001]
10. Lu R, et al. *Nature*. 2009; 462:358–362. [PubMed: 19924215]
11. Ow SY, et al. *J Proteome Res*. 2009; 8:5347–5355. [PubMed: 19754192]
12. Wenger CD, Phanstiel DH, Lee MV, Bailey DJ, Coon JJ. *Proteomics*. 2011; 11:1064–1074. [PubMed: 21298793]
13. Reid GE, Shang H, Hogan JM, Lee GU, McLuckey SA. *J Am Chem Soc*. 2002; 124:7353–7362. [PubMed: 12071744]
14. Liang X, McLuckey SA. *J Am Soc Mass Spectrom*. 2007; 18:882–890. [PubMed: 17349802]
15. McAlister GC, Phanstiel DH, Brumbaugh J, Westphall MS, Coon JJ. *Mol Cell Proteomics*. 2011; 10:O111 009456. [PubMed: 21393638]
16. Ludwig TE, et al. *Nat Methods*. 2006; 3:637–646. [PubMed: 16862139]
17. Lee MV, et al. *Mol Syst Biol*. 2011; 7:514. [PubMed: 21772262]
18. Martin SE, Shabanowitz J, Hunt DF, Marto JA. *Anal Chem*. 2000; 72:4266–4274. [PubMed: 11008759]
19. Geer LY, et al. *J Proteome Res*. 2004; 3:958–964. [PubMed: 15473683]
20. Elias JE, Gygi SP. *Nat Methods*. 2007; 4:207–214. [PubMed: 17327847]
21. Cherry JM, et al. *Nucleic Acids Res*. 1998; 26:73–79. [PubMed: 9399804]
22. Kersey PJ, et al. *Proteomics*. 2004; 4:1985–1988. [PubMed: 15221759]

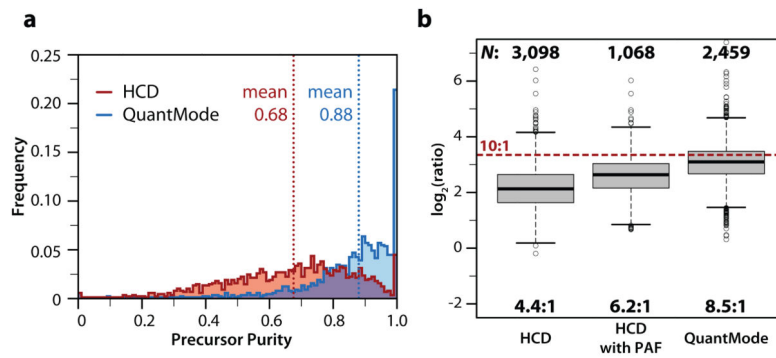


Figure 1.

Analysis of the *precursor purity model* and *quantitative accuracy model* samples with either HCD MS/MS or QuantMode. **(a)** Distribution of precursor purity as measured by examining reporter tag 126 (yeast) and 131 (human) for yeast-identified sequences using either HCD MS/MS (red) or QuantMode (blue). **(b)** Analysis of quantitative accuracy via HCD MS/MS (left), HCD MS/MS with PAF (middle), and QuantMode (right). The dashed red horizontal line indicates the true ratio while boxplots indicate the median (stripe), the 25th to 75th percentile (interquartile range, box), 1.5 times the interquartile range (whiskers), and outliers (open circles). The number of quantified yeast PSMs (N) and median ratio are given for each method.

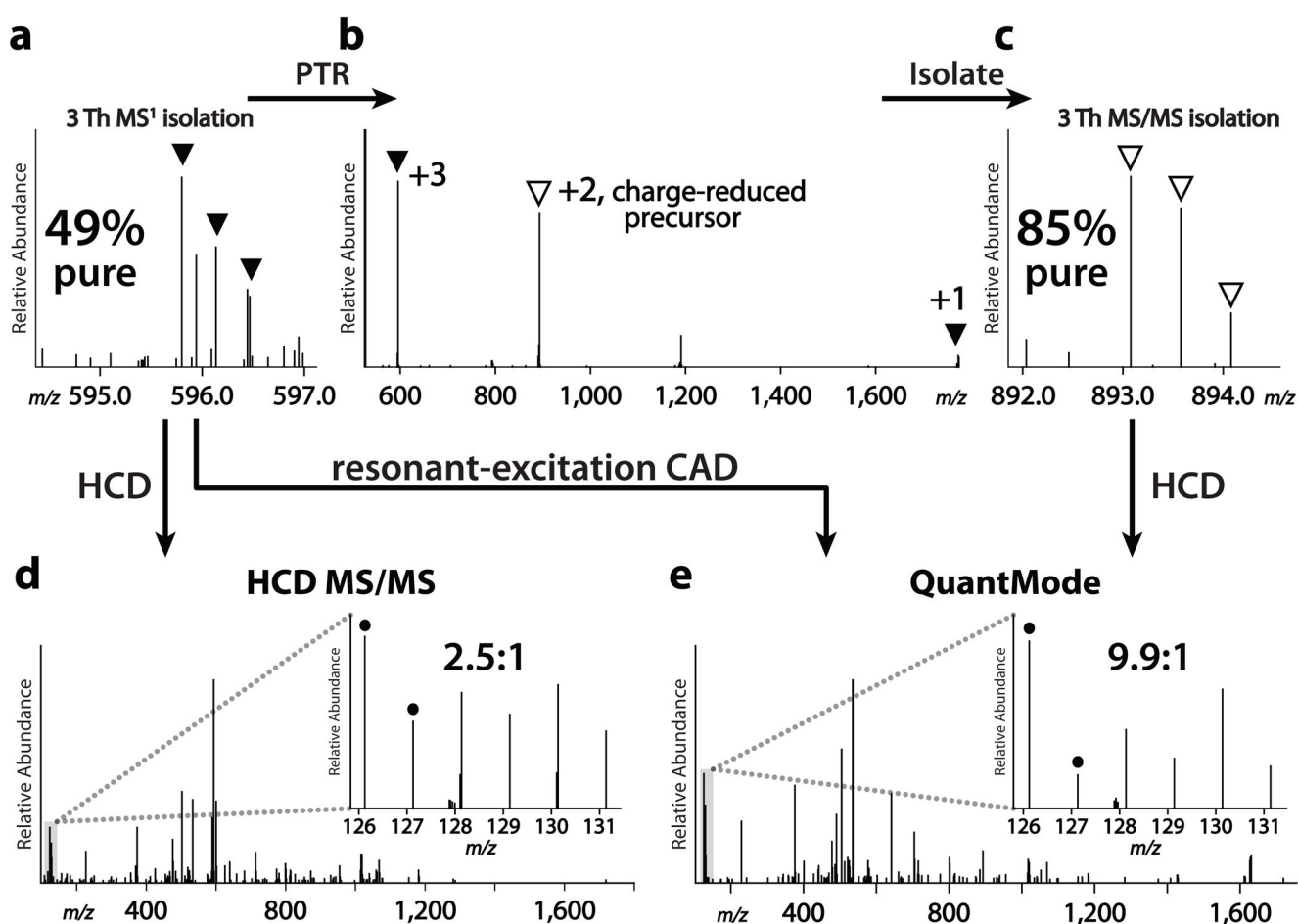


Figure 2.

Pedagogical overview of QuantMode. A triply charged precursor at m/z 595.72 was isolated with a 3 Th window (a). The precursor isotopic cluster occupies only 49% of the total ion current in this region. QuantMode begins with PTR (b); isolation of the charge-reduced precursor (+2) purifies this target to 85% (c); HCD converts these purified precursors to reporter ions; resonant-excitation CAD follows re-injection/re-isolation of the triply charged precursor. The HCD and CAD products are combined in the c-trap prior to orbitrap mass analysis. The conventional HCD MS/MS scan for this impure precursor (d) is juxtaposed against this QuantMode scan (e). Insets display the reporter ion region (identical intensity scale) and the quantitative accuracy achieved by both approaches for the 10:1 ratio.